

Comparative PSII photochemistry of quinoa and maize under mild to severe drought stress

C. MALAN and J.M. BERNER⁺ 

North-West University, Unit for Environmental Sciences and Management, Potchefstroom, South Africa

Abstract

Quinoa has been identified as a climate-resilient crop that can overcome unfavorable conditions. This study explores the photochemical efficiency of quinoa compared to maize subjected to drought stress. The JIP-test was used to assess the photochemical efficiency of both crops. Proline content, leaf water potential, and membrane leakage were also determined. The maximum photochemical efficiency (F_v/F_m) did not change for quinoa and maize under moderate stress. However, severe drought conditions resulted in a decline in F_v/F_m in maize but not quinoa. Furthermore, the PSII performance index ($PI_{ABS, total}$) declined steadily in maize soon after the onset of drought stress. The decline in the $PI_{ABS, total}$ values for quinoa was only observed after a period of severe drought stress. Membrane leakage was also more prevalent in the maize plants, while quinoa had higher proline contents. This study concluded that both quinoa and maize maintained PSII structure and function under moderate drought conditions. However, only quinoa maintained PSII structure and function under severe drought conditions.

Keywords: drought; leaf water potential; membrane leakage; performance index; photosynthesis; quantum yield.

Introduction

Plant productivity is dependent on the process of photosynthesis and consequently on the efficiency of the plant to use the available water (Sharma *et al.* 2019). During water-deficit conditions, the stomata of the plants close to prevent excessive water loss (Qi *et al.* 2018). However, the closing of the stomata also means that CO_2 cannot enter the plant. Therefore, the CO_2 supply for the carbon-reduction cycle becomes limited and reduces the

synthesis of assimilation products (Wang *et al.* 2018). Consequently, the demand for ATP and NADPH from the light-dependent (photochemical) phase of photosynthesis declines, causing the over-reduction of the photosynthetic electron transport chain (Logan *et al.* 2014). As a result, the production of reactive oxygen species is triggered, leading to the photooxidation of the PSII core subunit D1 and the oxygen-evolving complex (Henmi *et al.* 2004). Damage to the subunits will sequentially lead to the downregulation of electron flow (Aro *et al.* 1993).

Highlights

- PSII of maize and quinoa maintained structure and function under moderate drought stress
- PSII of quinoa maintained structure and function under severe drought stress but not maize
- High proline content is associated with quinoa drought tolerance

Received 3 November 2021

Accepted 11 April 2022

Published online 27 May 2022

⁺Corresponding author

e-mail: jacques.berner@nwu.ac.za

Abbreviations: ABS/RC = $(M_0/V_J)/\phi P_0$ – effective antenna size of active reaction centers; DI₀/RC = ABS/RC – TR₀/RC – heat dissipation per reaction center; DM – dry mass; ET₀/RC = $(M_0/V_J) \times \psi E_0$ – electron transport per reaction center; F₀/F_m – heat dissipation of the PSII antenna; FM – fresh mass; F_v/F_m – maximal quantum yield of PSII photochemistry; OEC – oxygen-evolving complex; PI_{ABS} = $(RC/ABS) \times [\phi P_0/(1 - \phi P_0)] \times [\psi E_0/(1 - \psi E_0)]$ – performance index based upon absorption; PI_{ABS, total} = PI_{ABS} $\times [\delta R_0/(1 - \delta R_0)]$ – total performance index; RC – reaction center; RWC – relative water content; TM – turgid mass; TR₀/RC = M_0/V_J – trapping per reaction center; W – watered; WD – water deficit.

Acknowledgments: This work was supported by the National Research Foundation (NRF) in collaboration with the German Academic Exchange Service (DAAD) (109733).

Conflict of interest: The authors declare that they have no conflict of interest.

Physiological responses of plants to drought stress are very complicated and vary among plant species, along with the degree and duration of drought exposure (Anjum *et al.* 2011). Generally, C₄ plants, such as maize, are less susceptible to drought stress when compared to a C₃ species. This advantage is attributed to the different morphological, anatomical, and biochemical mechanisms used during carbon fixation in C₃ and C₄ species (Pearcy and Ehleringer 1984). C₄ species can increase energy consumption efficiency through energy conservation and thereby maintain a higher photosynthetic performance and water-use efficiency than C₃ species under water-stress conditions (Majeran *et al.* 2010, Petrova *et al.* 2020). While water stress can lead to an excess of energy absorbed by the leaves associated with altered CO₂ assimilation, C₄ species tend to be better adapted to high light and temperature intensities than C₃ species (Guidi *et al.* 2019).

Chlorophyll *a* fluorescence measurements are widely used as a rapid, accurate, and nondestructive probe to study PSII photochemistry (Hagen *et al.* 2006). In addition, the fluorescence induction curve analysis provides a vast amount of data to study the plant's response to environmental stress (Strasser *et al.* 2004). Various studies have indicated that the functional activity and structural stability of PSII are susceptible to drought stress (Meng *et al.* 2016). The drought period's intensity and duration seem to significantly influence PSII photochemistry (Xu *et al.* 2010). PSII is damaged under severe water stress conditions at both the donor and acceptor ends (Bano *et al.* 2021).

To fully understand the photosynthetic tolerance of C₃ and C₄ species to drought stress, the photochemical reactions need to be elucidated much more. Quinoa, a C₃ species, has a remarkable ability to tolerate drought conditions, which most other popular crops lack (González *et al.* 2015). The ability to tolerate drought conditions is associated with increased contents of osmoprotectants, maintaining photosynthesis under unfavorable conditions, and low water-use requirements (Azurita-Silva *et al.* 2015). When maize is subjected to drought stress, the photosynthetic efficiency of maize declines (Liu *et al.* 2018). As a result, this study compared the photochemical responses used by both quinoa and maize when subjected to water deficit stress. This was achieved by investigating quinoa and maize's photochemical efficiency and proline content while subjected to water stress.

Materials and methods

Growth conditions: The glasshouses' temperature regimes were set at 30°C for the daytime and the night temperatures were at 16°C. The day length was set to 13 h using fluorescent growth light tubes. The photosynthetic active radiation (PAR) during the day ranged between 600 and 800 μmol(photon) m⁻² s⁻¹ (Malan 2020).

Plant cultivation: Quinoa (*Chenopodium quinoa* Willd) seeds, as well as maize seeds, were planted in 2-L pots containing *Hygromix*® (Hygrotech, RSA) and soil (3:2 mixture). A controlled-release fertilizer (*Osmocote Pro* for

3–4 months), with an NPK ratio of 17:11:10, was used to fertilize the pots before planting (Malan 2020).

Water regimes: Two water regimes were used during this trial, namely a well-watered and a water-stressed treatment. The plants were watered twice a day until the seedlings were established. The water stress treatment was started four weeks after emergence (vegetative stage). *Decagon*® soil moisture sensors GS3 were placed in selected pots to measure the hourly soil moisture status. The water stress conditions were maintained until the soil water content reached 0.01 m³ m⁻³. At this point, the water stress treatment was stopped (Malan 2020).

Chlorophyll (Chl) *a* fluorescence: The kinetics of the polyphasic prompt fluorescence rise was measured *in vivo* using the *M-PEA* fluorimeter (Hansatech Instrument Ltd., King's Lynn, Norfolk, UK). Plants were dark-adapted for 1 h before the start of the measurement. Measurements were taken at five different spots on the adaxial surface of the fully developed canopy leaves. Chl *a* fluorescence measurements were recorded after illumination by a red actinic light of 3,000 μmol(photon) m⁻² s⁻¹ provided by three light-emitting diodes with a 5-mm diameter focus spot and 12-bit resolution in 1 s. The *M-PEA* fluorimeter data set points were set at 0.02 ms to 0.05 ms for the initial fluorescence O step; intermediate steps J at 2 ms and I at 30 ms, and peak P step at 300 ms. *M-PEA Plus* (v. 1.10) software was used to calculate the photosynthetic (OJIP) parameters from the variable fluorescence. The theory of energy flow in thylakoid membranes describes photosynthetic pigment inflow and outflow energy, forming the basis of the JIP-test (Kalaji *et al.* 2017, 2018). According to the JIP-test, the primary factor controlling Chl emission is the redox state of Q_A; the more Q_A is reduced, the higher the Chl rise. Lazár (2006), however, summarized that this is not the only process that causes Chl alterations, and that many other processes have been proposed to do so as well.

Due to physical and chemical environmental conditions, the plant's physiological state will determine the shape of the OJIP transient (Digrado *et al.* 2017, Banks 2018, Pšidová *et al.* 2018). To survive, the plant needs to adapt to these stress conditions; therefore, the ability to adapt is studied through the vitality of the plant's photosynthetic system (Guo *et al.* 2008, Longenberger *et al.* 2009, Kalaji *et al.* 2017). The JIP-test allows a separate estimation of the maximum yield of primary photochemistry. It also examines the probability that an electron would move into the electron transport chain beyond Q_A⁻ (quinone A). Therefore, the OJIP transient represents the reduction of the electron transport chain. The OJIP curves can, therefore, be used to analyze how efficiently the plant photosynthesizes under conditions of stress (Malan 2020). Several parameters based on the OJIP transient were measured in this study (Appendix).

Membrane leakage: Three 10-mm discs were sampled per plant with a cork borer. The leaf discs were rinsed three times to remove excess electrolytes and placed in separate

tubes containing 10 mL of deionized water. Hereafter, the samples were placed in the dark for 24 h, after which the initial ionic leakage was measured with an EC meter (*Primo 5, HANNA Instruments, USA*). The samples were then autoclaved for 20 min to dissociate all cellular cytosols into a solution. The final ionic leakage was measured after the samples were cooled to room temperature, and calculations were performed as an injury index percentage at 100°C (*Sullivan 1971*): $ML = 1 - (\text{final} - \text{initial})/\text{initial} \times 100$, where 'final' and 'initial' represent the membrane leakage measurements.

Relative water content: Cut leaf discs were approximately 1.5 cm in diameter and prominent veins were avoided (*Barrs and Weatherley 1962*). The leaf discs were weighed to obtain the initial mass. At room light and temperature, the leaf discs were immediately hydrated to full turgidity for 3–4 h. Leaf discs were hydrated by floating on deionized water in a closed Petri dish. The samples were taken out of the water, dried rapidly with tissue paper, and weighed to get the turgid mass. The leaf discs' dry mass was obtained after drying the leaves in an oven for 24 h at 80°C (*Malan 2020*). The relative water content (RWC) was determined as: $RWC [\%] = [(FM - DM)/(TM - DM)] \times 100$, where FM is the fresh mass, DM is the dry mass, and TM is the turgid mass (*Barrs and Weatherley 1962*).

Proline content: As *Carillo and Gibon (2011)* described, the ninhydrin method was used to determine the free proline content in both quinoa and maize leaves (*Malan 2020*). The proline was extracted from the leaf tissue using 40% ethanol and an acidic ninhydrin solution. The samples were placed in a block heater at 95°C for 20 min. Hereafter, the absorbance was measured at 520 nm with a *Shimadzu UV-1800 UV-Vis spectrophotometer* (Kyoto, Japan). A calibration curve was made with known concentrations ranging from 0.04 to 1 mM. Thus, the proline content typically ranges from 0.5 (unstressed) to 50 (stressed) $\mu\text{mol g}^{-1}(\text{FM})$ (*Carillo and Gibon 2011*).

Statistical analysis: All experiments were repeated at least eight times. Statistical analysis was implemented using *SigmaPlot v. 12.0* software (*Systat Software, Inc., San Jose, California, USA*). Data sets with parametric distribution and differences between treatments were subjected to a one-way analysis of variance (*ANOVA*) to compare treatments at the 5% significance level (*Tukey's test*).

Results

OJIP fluorescence transient: Acute water deficit conditions resulted in a significant decline in the maize plants' OJIP transient at a soil moisture content of 0.1 $\text{m}^3 \text{ m}^{-3}$. A drop in the OJIP transient of the maize water-deficit treatment was evident from 1 ms. In contrast, a decline in the other treatments can be seen from 30 ms (Fig. 1A). The OJIP transient of the quinoa water deficit treatment was significantly lower when compared to the watered treatments but considerably higher than the maize water deficit treatment (Fig. 1A).

Relative variable fluorescence: To unveil hidden information within the OJIP transients, the difference in variable fluorescence was double normalized and plotted on a logarithmic time scale (*Malan 2020*). The efficiency of the movement of electrons through the photosynthetic electron chain can be further assessed by plotting the different bands. Under severe water stress, quinoa displayed $+\Delta V_K$, $+\Delta V_J$, ΔV_I , and $-\Delta V_G$ bands, whereas the water-stressed maize displayed $+\Delta V_K$, $+\Delta V_J$, and $-\Delta V_G$ bands (Fig. 1B–D). The magnitude of the bands was higher in the maize water-stressed plants.

Pool size of the end electron acceptors: To further investigate the impact of the water stress on the I–P phase, these transients were normalized between 30 ms and 300 ms and plotted on a logarithmic time scale (Fig. 2). A significant decrease in the pool size of the end electron acceptors was observed in both the quinoa and water-stressed plants compared to their respective controls. However, the water-stressed maize plants had a significantly smaller pool of end electron acceptors than the quinoa water-stressed plants (*Malan 2020*).

Photosynthetic parameters: No statistical differences were observed in the F_v/F_m values of the quinoa plants subjected to water-stressed conditions. With values ranging between 0.81 and 0.83. However, a gradual decline in the F_v/F_m values was observed when maize plants were subjected to water-stressed conditions reaching a value of 0.55 under severe water-stressed conditions. (Fig. 3A). A statistical decline in the $PI_{ABS,\text{total}}$ of quinoa was only observed after 11 d of withholding water. In contrast, maize showed a decrease in the $PI_{ABS,\text{total}}$ values right from the onset of the water stress (Fig. 3B). The amount of energy dissipated by the PSII antenna, F_0/F_m , of the maize plants under water-stressed conditions was significantly higher than of quinoa. The quinoa plants did not substantially increase the F_0/F_m values as the water-stressed conditions progressed (Fig. 4).

A 3.5-fold increase in the heat dissipation per reaction center (DI_0/RC) of the maize plants was observed, while quinoa only showed a 1.6-fold increase (Fig. 5). This increase in heat dissipation of the water-stressed maize plants coincided with an increase in the effective active antenna size of PSII (ABS/RC) and the trapping of light energy (TR_0/RC) (Fig. 5). A decrease in the density of the active reaction centers [$\gamma RC/(1 - \gamma RC)$], the maximum yield of primary photochemistry [$\phi P_0/(1 - \phi P_0)$] and the probability to move an electron further than Q_A^- [$\psi E_0/(1 - \psi E_0)$] was observed in both the maize and quinoa plants. Still, the decline was more prominent in the maize plants (Fig. 5). However, an increase in the probability of reducing an end electron acceptor [$\delta R_0/(1 - \delta R_0)$] was observed in the maize stressed plants (Fig. 5).

Proline, membrane leakage, leaf water potential, and biomass: A statistical increase in membrane leakage was observed in both the quinoa and maize plants under extreme water stress conditions (Fig. 6A). However, membrane leakage was considerably lower in the water-

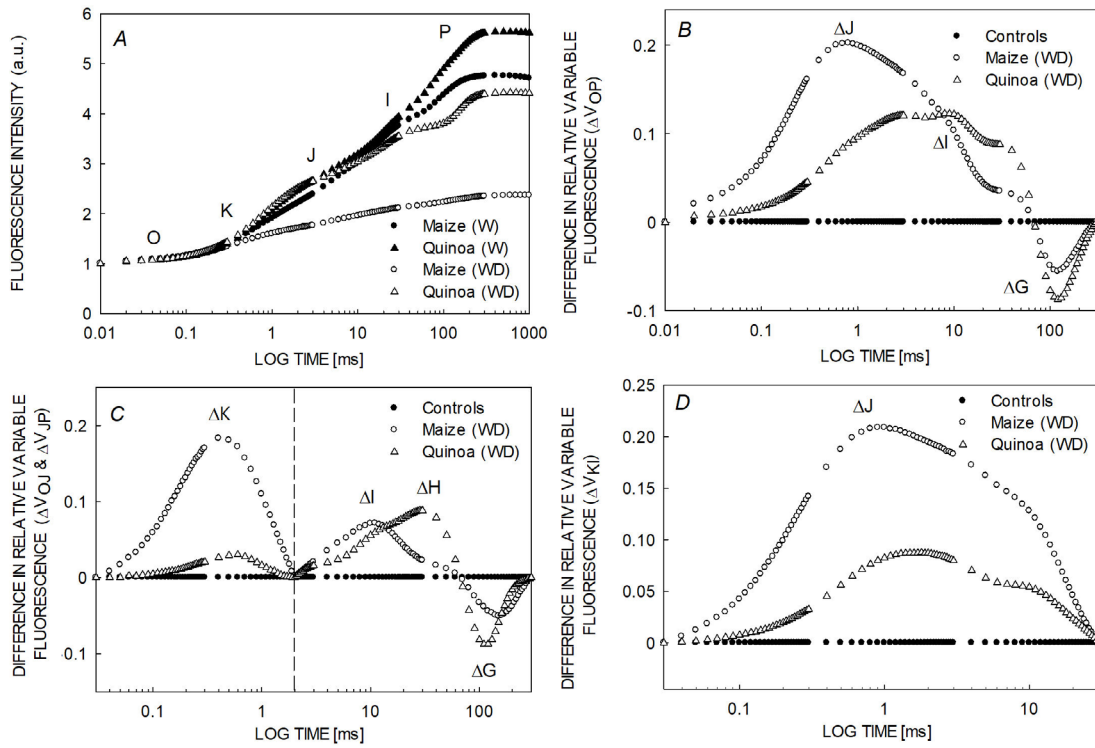


Fig. 1. Photochemical responses of quinoa and maize to extreme water deficit ($0.01 \text{ m}^3 \text{ m}^{-3}$) conditions, assessed by means of fluorescence transient analysis. The average chlorophyll a fluorescence transient (OJIP) of dark-adapted leaves of quinoa and maize, normalized at 0.03 ms and plotted on a logarithmic time scale (A). Difference in relative variable fluorescence (ΔV) curves of intact leaves were obtained by subtraction ($V_{\text{treatment}} - V_{\text{control}}$) of the original fluorescence transients, normalized between 0.03 ms and 300 ms (B), 0.03 ms and 2 ms (C), 2 ms and 300 ms (D). WD – water deficit; W – watered.

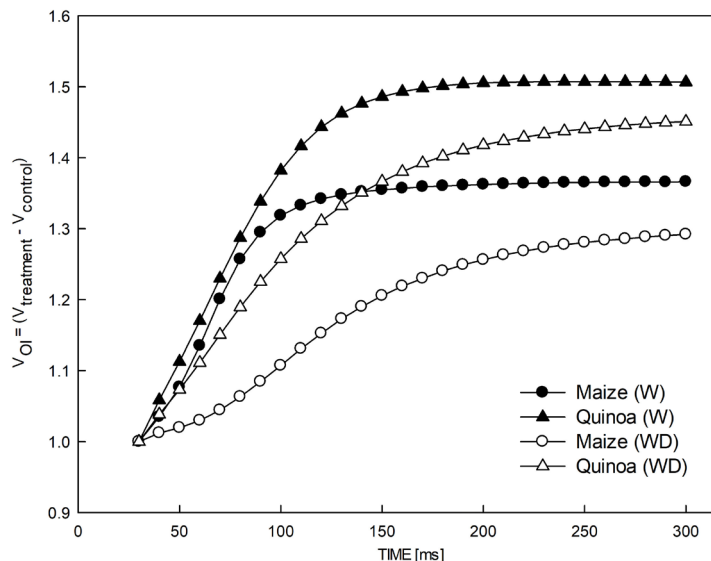


Fig. 2. Variable fluorescence ($\Delta V_{\text{OI}} = V_{\text{treatment}} - V_{\text{control}}$), normalized between 30 μs and 300 ms, of intact quinoa and maize leaves subjected to extreme water deficit stress. WD – water deficit; W – watered.

stressed quinoa than that in the water-stressed maize (Fig. 6A). The leaf water content of both the quinoa and maize plants dropped significantly, but there were no significant differences in the water content of quinoa and maize under water stress (Fig. 6B). No significant differences were found in the dry biomass between the water-stressed quinoa and the well-watered quinoa.

However, significant differences were found in the dry biomass between the water-stressed maize and the well-watered maize (Fig. 6C). A 17.4% difference in the dry biomass was found between the water-stressed quinoa and the well-watered quinoa. The dry mass of water-stressed maize decreased by 40.1% in comparison to the well-watered maize (Fig. 6C). The proline content of

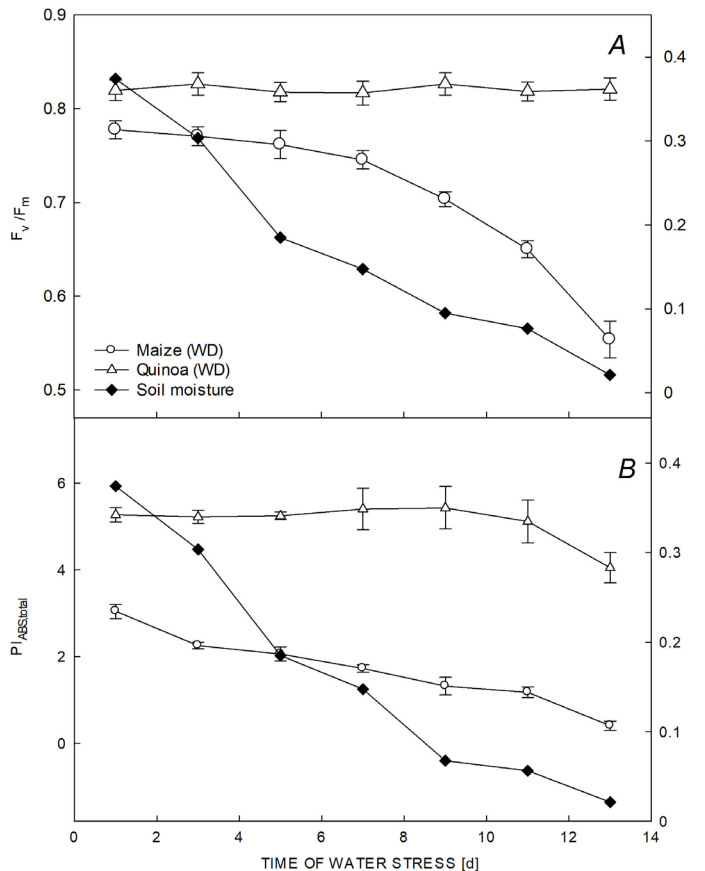


Fig. 3. Changes in the maximum quantum efficiency (F_v/F_m) of PSII (A) and the performance index ($PI_{ABS, total}$) (B) of maize and quinoa over time in response to a declining soil moisture content. WD – water deficit. Values represent averages \pm SD, $n = 5$.

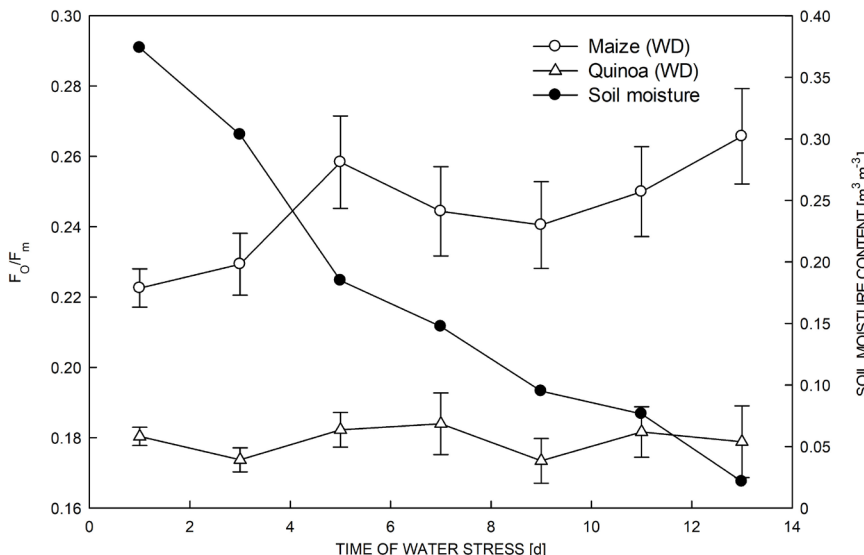


Fig. 4. Changes in the heat dissipation of the PSII antenna (F_0/F_m) values of maize and quinoa over time in response to a declining soil moisture content. WD – water deficit. Values represent averages \pm SD, $n = 5$.

both quinoa and maize increased drastically under severe water stress (Fig. 6D). However, the water-stressed quinoa had significantly higher proline contents than the water-stressed maize.

Discussion

The adaptability of crops to changes in the environment is a crucial survival mechanism. Optimal photosynthesis

under adverse conditions is a determining factor for the plants' successful adaptability (Athaniou *et al.* 2010). Because photosynthesis is vital for plant survival, both quinoa and maize's PSII photochemical efficiency was investigated under water deficit conditions.

Since maize is a C₄ plant, it is assumed that maize would be less susceptible to photoinhibition and photodamage under water stress conditions when compared to quinoa, a C₃ species. On the contrary, this investigation

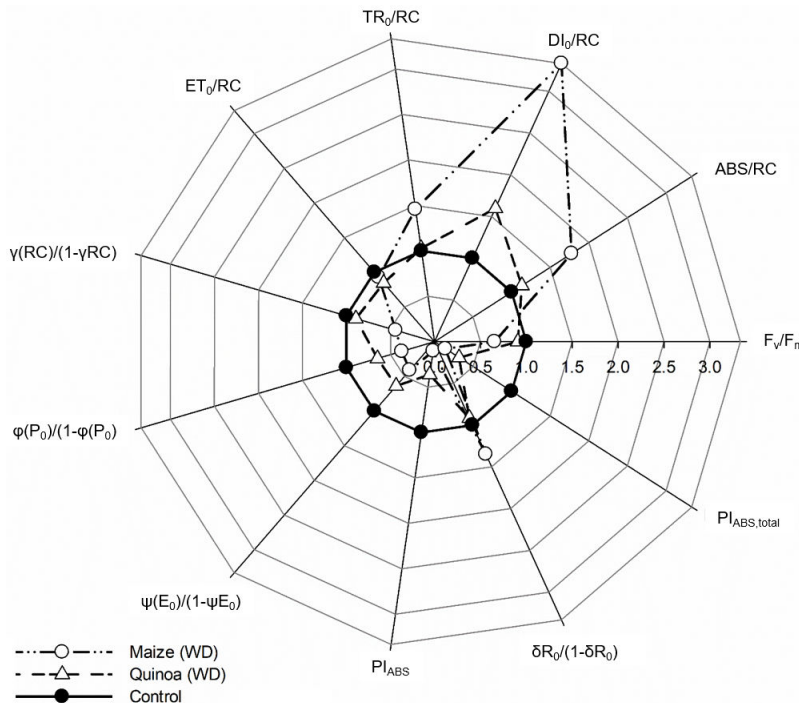


Fig. 5. Fractional changes in selected functional and structural parameters of PSII relative to the control treatments of both quinoa and maize subjected to extreme water deficit conditions; volumetric soil water content of $0.01 \text{ m}^3 \text{ m}^{-3}$. The treatments were normalized according to their relevant controls and plotted on a multiparametric radar plot. WD – water deficit; W – watered.

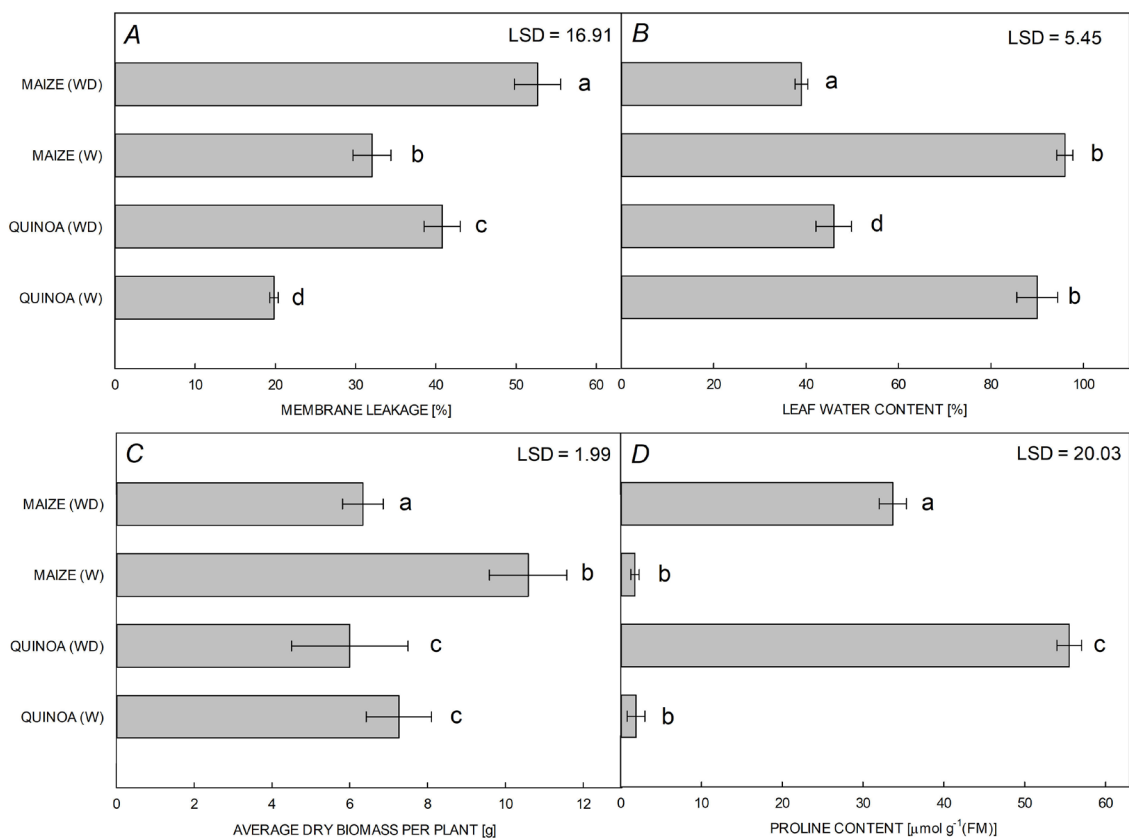


Fig. 6. Membrane leakage (A), leaf water content (B), dry mass per plant (C), and proline content (D) of both quinoa and maize under conditions of severe water stress; volumetric soil water content of $0.01 \text{ m}^3 \text{ m}^{-3}$. Treatment values not connected by the same letters are significantly different ($P < 0.05$). WD – water deficit; W – watered. Values represent averages \pm SD, $n = 5$.

showed that quinoa's ability to acclimate to water-deficit conditions surpasses maize's. Maintaining a favorable electron flow during photochemistry is vital to quinoa's ability to withstand unfavorable conditions. In contrast, maize could not sustain a favorable electron flow during water-deficit stress.

PSII is sensitive to abiotic stress (Mathur *et al.* 2014, Guidi *et al.* 2019, Rane *et al.* 2021) and plants need to maintain homeostasis between environment and plant functionality (Gupta 2020). Severe drought conditions result in the inactivation of the OEC and reduce photochemical reactions (Souza *et al.* 2004). The inhibiting effect of water stress on electron movement between PSII and PSI was more noticeable in the maize plants than in the quinoa plants (Fig. 1). The development of the K band indicates a decrease in the functionality of the OEC complex (Strasser *et al.* 2007, Zhou *et al.* 2019), leading to an imbalance between the electron flow leaving the reaction center and moving towards the acceptor side and the electron flow coming towards the reaction center from the donor side of PSII (Yusuf *et al.* 2010, Bussotti *et al.* 2011, Chen *et al.* 2016, Kalaji *et al.* 2017, 2018). Water stress resulted in maize's K band being 3-fold higher than quinoa's K band (Fig. 1C). Because of the decrease in the functionality of maize's OEC, the supply of electrons from PSII was constrained. Furthermore, severe water stress resulted in the formation of a pronounced J band in the maize plants, indicating the accumulation of Q_A^- (Fig. 1D), which coincided with a decrease in the reduction in the pool size of the end electron acceptors (Fig. 2).

The accumulation of excess electrons in the electron transport chain can give rise to the formation of reactive oxygen species, which could damage PSII (Krieger-Liszka and Shimakawa 2022). Damage to PSII is identified by a decline in the F_v/F_m values (Badr and Brüggemann 2020). There was no statistical decline in the F_v/F_m values of quinoa, indicating that quinoa was able to protect PSII from photodamage (Fig. 3A). In contrast, a decrease in the F_v/F_m values was observed in maize even under moderate water stress.

The PI_{ABS} and the $PI_{ABS, total}$ performance indexes can evaluate the overall plant performance. These indexes are helpful because they consider the plant's ability to absorb sunlight energy, the trapping of the absorbed energy, and the probability of moving electrons further than Q_A (Kalaji *et al.* 2017). Also, the calculations for the $PI_{ABS, total}$ include the likelihood of reducing the end electron acceptors. The ability of quinoa to maintain much higher PI_{ABS} and $PI_{ABS, total}$ (Fig. 5) values under drought stress, compared to maize, indicates the potential of the plant to support photosynthesis under adverse conditions. In addition, quinoa had a considerably higher PI_{ABS} compared to the maize throughout the water stress trial. This suggests that the water-stressed quinoa had higher photochemical efficiency compared to water-stressed maize.

The dissipation of heat energy from the active reaction centers (DI_0/RC) increased significantly (Fig. 5) for the water-stressed maize when compared to the well-watered maize, which coincided with the increase in the effective antenna size of active RCs (ABS/RC) (Fig. 5). The high

amount of energy lost in the form of heat dissipation (DI_0/RC) (energy that is not utilized by photosynthesis) indicated that the maize plants were subjected to stress (Lauriano *et al.* 2006, Kalaji *et al.* 2017). Compared to its corresponding well-watered treatment, the density of active RCs of maize plants decreased significantly under water-stress conditions.

Singlet oxygen production is promoted if the antenna complexes deliver too much energy under water-stress conditions. This causes photooxidative damage in the thylakoid membranes of the chlorophyll pigments and irreversible peroxidation of membrane lipids (Kalaji *et al.* 2016, 2017). Several studies have been identified with similar results regarding the effect of water stress on *Calluna vulgaris* (Albert *et al.* 2011), tomato plants (Zushi *et al.* 2012), and maize (Liu *et al.* 2018). On the other hand, under drought conditions, quinoa reduced the amount of energy trapped per reaction center (TR_0/RC) as well as reduced electron transport per reaction center (ET_0/RC) (Fig. 5). As an acclimation strategy, the active reaction centers were converted into inactive reaction centers, reducing the trapping efficiency and PSII activity.

The decrease influenced the downregulation of PSII in the ability to absorb light energy [$\gamma RC/(1 - \gamma RC)$], a decreased trapping of excitation energy (TR_0/RC), and a decrease in the movement of electrons between the reaction centers and Q_A [$\psi E_0/(1 - \psi E_0)$] (Fig. 5). This observation was found for both the water-stressed quinoa and maize treatments compared to the respective controls. The PSII activity of the water-stressed maize decreased significantly compared to the water-stressed quinoa.

Compared to the control, the water-stressed quinoa had a significantly higher ability to reduce the end electron acceptors at the PSI acceptor side [$\delta R_0/(1 - \delta R_0)$]. Therefore, the probability of reducing $NADP^+$ to $NADPH$ increased compared to its respective control treatment. In contrast, the water-stressed maize's ability to reduce $NADP^+$ to $NADPH$ decreased significantly compared to the control treatments (Fig. 5).

Plant growth slows under water deficit conditions, and as a result, the demand for carbohydrates from photosynthesis declines (Rodrigues *et al.* 2019). However, from an energy supply point of view, the same amount of energy is absorbed by the plant, but less energy is utilized. Therefore, if the plant fails to dissipate the absorbed excess energy, photoinhibition will cause extensive damage.

A vital response of plants to stress conditions is the accumulation of compatible osmolytes such as proline. Several studies have illustrated the importance of proline in response to drought stress (Hayat *et al.* 2012, Furlan *et al.* 2020, Semida *et al.* 2020). Though quinoa and maize accumulated proline in response to water-deficit stress, quinoa accumulated more proline than maize. Proline functions as an osmoprotectant, stabilizing cellular structures, enzymes, and scavenging reactive oxygen species (Meena *et al.* 2019). Proline accumulates in the chloroplast, where it protects the photosynthetic machinery to sustain a favorable redox balance. By doing so, a favorable content of $NADPH$ is maintained (Oukarroum *et al.* 2012). The high proline contents of quinoa helped

protect the photosynthetic machinery against oxidative damage, ensuring the plant's ability to reduce NADP^+ to $\text{NADPH} [\delta\text{R}_0/(1 - \delta\text{R}_0)]$. Where crops could not accumulate proline under water-deficit conditions, severe damage to the crops was observed (Slama *et al.* 2015).

Previous studies suggested that proline protects the OEC under water deficit stress (De Ronde *et al.* 2004, Oukarroum *et al.* 2012, Rejeb *et al.* 2014, Chen *et al.* 2016) by stabilizing the Mn cluster (Allakhverdiev *et al.* 1996) and by detoxifying free radicals that result from photoinhibition. The increased proline contents in the water-stressed quinoa assisted in protecting the photosynthetic complexes by minimizing the oxidative damage to these systems. Quinoa's potential to protect its membranes is reflected by the lower membrane leakage percentage (Fig. 6A). Maize's inability to protect its membranes will ultimately lead to insufficient photosynthesis and reduced growth (Fig. 6C).

Quinoa was able to tolerate the water-stressed conditions more successfully compared to the water-stressed maize. The higher proline contents in the water-stressed quinoa also indicate an increase in the tolerance of PSII during water-stressed conditions. The water-stressed quinoa produced more proline, thereby protecting the OEC and increasing electrons' flow between PSII and PSI. With increasing temperature, quinoa, therefore, could acclimatize more efficiently compared to maize. The water-stressed maize's inability to tolerate drought stress, drastically downregulated maize's photochemical efficiency, thereby lowering plant performance.

Conclusion: As C_3 species, quinoa could adapt more successfully to the abiotic stress than maize, a C_4 species. This was observed by the water-stressed quinoa's ability to accumulate a higher concentration of proline, thereby increasing the tolerance of PSII to the water deficit stress. As an acclimatization technique, quinoa reduced the degree of damage in the thylakoid membranes by converting active reaction centers to inactive reaction centers. As a result, the flow of electrons between PSII and PSI continued optimally. Unfortunately, the severity of the photodamage in the water deficit maize and the low contents of proline reduced the maize's ability to protect PSII. In this study, quinoa could acclimate more successfully to the water-stressed conditions than the water-stressed maize. Further research is needed to quantify water stress on PSI function as the gradients of PSI and PSII ratios differ substantially between C_3 and C_4 species.

References

Albert K.R., Mikkelsen T.N., Michelsen A. *et al.*: Interactive effects of drought, elevated CO_2 and warming on photosynthetic capacity and photosystem performance in temperate heath plants. – *J. Plant Physiol.* **168**: 1550-1561, 2011.

Allakhverdiev S.I., Feyziev Y.M., Ahmed A. *et al.*: Stabilization of oxygen evolution and primary electron transport reactions in photosystem II against heat stress with glycinebetaine and sucrose. – *J. Photoch. Photobio. B* **34**: 149-157, 1996.

Anjum S.A., Xie X., Wang L. *et al.*: Morphological, physiological and biochemical responses of plants to drought stress. – *Afr. J. Agr. Res.* **6**: 2026-2032, 2011.

Aro E.-M., Virgin I., Andersson B.: Photoinhibition of Photosystem II. Inactivation, protein damage and turnover. – *BBA-Bioenergetics* **1143**: 113-134, 1993.

Athanasiou K., Dyson B.C., Webster R.E., Johnson G.N.: Dynamic acclimation of photosynthesis increases plant fitness in changing environments. – *Plant Physiol.* **152**: 366-373, 2010.

Azurita-Silva A., Jacobsen S.-E., Razzaghi F. *et al.*: Quinoa drought responses and adaptation. – In: Bazile D., Bertero D., Nieto C. (ed.): *State of the Art Report of Quinoa in the World in 2013*. FAO and CIRAD, Rome 2015.

Badr A., Brüggermann W.: Comparative analysis of drought stress response of maize genotypes using chlorophyll fluorescence measurements and leaf relative water content. – *Photosynthetica* **58**: 638-645, 2020.

Banks J.M.: Chlorophyll fluorescence as a tool to identify drought stress in *Acer* genotypes. – *Environ. Exp. Bot.* **155**: 118-127, 2018.

Bano H., Habib-ur-Rehman A., Zafar Z.U. *et al.*: Linking changes in chlorophyll *a* fluorescence with drought stress susceptibility in mung bean [*Vigna radiata* (L.) Wilczek]. – *Physiol. Plantarum* **172**: 1244-1254, 2021.

Barrs H.D., Weatherley P.E.: A re-examination of the relative turgidity technique for estimating water deficits in leaves. – *Aust. J. Biol. Sci.* **15**: 413-428, 1962.

Busotti F., Desotgiu R., Cascio C. *et al.*: Ozone stress in woody plants assessed with chlorophyll *a* fluorescence. A critical reassessment of existing data. – *Environ. Exp. Bot.* **73**: 19-30, 2011.

Carillo P., Gibon Y.: PROTOCOL: Extraction and determination of proline. – Prometheus Wiki, 2011.

Chen Y.E., Liu W.J., Su Y.Q. *et al.*: Different response of photosystem II to short and long-term drought stress in *Arabidopsis thaliana*. – *Physiol. Plantarum* **158**: 225-235, 2016.

De Ronde J.A., Cress W.A., Krüger G.H.J. *et al.*: Photosynthetic response of transgenic soybean plants, containing an *Arabidopsis P5CR* gene, during heat and drought stress. – *J. Plant Physiol.* **161**: 1211-1224, 2004.

Digrado A., Bachy A., Mozaffar A. *et al.*: Long-term measurements of chlorophyll *a* fluorescence using the JIP-test show that combined abiotic stresses influence the photosynthetic performance of the perennial ryegrass (*Lolium perenne*) in a managed temperate grassland. – *Physiol. Plantarum* **161**: 355-371, 2017.

Furlan A.L., Bianucci E., Giordano W. *et al.*: Proline metabolic dynamics and implications in drought tolerance of peanut plants. – *Plant Physiol. Bioch.* **151**: 566-578, 2020.

González J.A., Eisa S.S.S., Hussin S.A.E.S., Prado F.E.: Quinoa: An incan crop to face global changes in agriculture. – In: Murphy K., Matanguihan J. (ed.): *Quinoa: Improvement and Sustainable Production*. Pp. 1-18. John Wiley & Sons, Inc., Hoboken 2015.

Guidi L., Lo Piccolo E., Landi M.: Chlorophyll fluorescence, photoinhibition and abiotic stress: Does it make any difference the fact to be a C_3 or C_4 species? – *Front. Plant Sci.* **10**: 174, 2019.

Guo P., Baum M., Varshney R.K. *et al.*: QTLs for chlorophyll and chlorophyll fluorescence parameters in barley under post-flowering drought. – *Euphytica* **163**: 203-214, 2008.

Gupta R.: The oxygen-evolving complex: a super catalyst for life on earth, in response to abiotic stresses. – *Plant Signal. Behav.* **15**: 1824721, 2020.

Hagen S.F., Solhaug K.A., Bengtsson G.B. *et al.*: Chlorophyll

fluorescence as a tool for non-destructive estimation of anthocyanins and total flavonoids in apples. – *Postharvest Biol. Tec.* **41**: 156-163, 2006.

Hayat S., Hayat Q., Alyemeni M.N. *et al.*: Role of proline under changing environments: a review. – *Plant Signal. Behav.* **7**: 1456-1466, 2012.

Henmi T., Miyao M., Yamamoto Y.: Release and reactive-oxygen-mediated damage of the oxygen-evolving complex subunits of PSII during photoinhibition. – *Plant Cell Physiol.* **45**: 243-250, 2004.

Kalaji H.M., Jajoo A., Oukarroum A. *et al.*: Chlorophyll *a* fluorescence as a tool to monitor physiological status of plants under abiotic stress conditions. – *Acta Physiol. Plant.* **38**: 102, 2016.

Kalaji H.M., Račková L., Paganová V. *et al.*: Can chlorophyll-*a* fluorescence parameters be used as bio-indicators to distinguish between drought and salinity stress in *Tilia cordata* Mill? – *Environ. Exp. Bot.* **152**: 149-157, 2018.

Kalaji H.M., Schansker G., Brestic M. *et al.*: Frequently asked questions about chlorophyll fluorescence, the sequel. – *Photosynth. Res.* **132**: 13-66, 2017.

Krieger-Liszka A., Shimakawa G.: Regulation of the generation of reactive oxygen species during photosynthetic electron transport. – *Biochem. Soc. T.* **50**: 1025-1034, 2022.

Lauriano J.A., Ramalho J.C., Lidon F.C., do Céu Matos M.: Mechanisms of energy dissipation in peanut under water stress. – *Photosynthetica* **44**: 404-410, 2006.

Lazár D.: The polyphasic chlorophyll *a* fluorescence rise measured under high intensity of exciting light. – *Funct. Plant Biol.* **33**: 9-30, 2006.

Liu J., Guo Y.Y., Bai Y.W. *et al.*: Effects of drought stress on the photosynthesis in maize. – *Russ. J. Plant Physiol.* **65**: 849-856, 2018.

Logan B.A., Demmig-Adams B., Adams III W.W., Bilger W.: Context, quantification, and measurement guide for non-photochemical quenching of chlorophyll fluorescence. – In: Demmig-Adams B., Garab G., Adams III W.W., Govindjee (ed.): *Non-Photochemical Quenching and Energy Dissipation in Plants, Algae and Cyanobacteria. Advances in Photosynthesis and Respiration*. Vol. 40. Pp. 187-201. Springer, Dordrecht 2014.

Longenberger P.S., Smith C.W., Duke S.E., McMichael B.L.: Evaluation of chlorophyll fluorescence as a tool for the identification of drought tolerance in upland cotton. – *Euphytica* **166**: 25-33, 2009.

Majeran W., Friso G., Ponnala L. *et al.*: Structural and metabolic transitions of C₄ leaf development and differentiation defined by microscopy and quantitative proteomics in maize. – *Plant Cell* **22**: 3509-3524, 2010.

Malan C.: Comparing the photochemical potential of quinoa to maize under water stress conditions. PhD Thesis. Pp. 135. North-West University, Potchefstroom 2020.

Mathur S., Agrawal D., Jajoo A.: Photosynthesis: Response to high temperature stress. – *J. Photoch. Photobio. B* **137**: 116-126, 2014.

Meena M., Divyanshu K., Kumar S. *et al.*: Regulation of L-proline biosynthesis, signal transduction, transport, accumulation and its vital role in plants during variable environmental conditions. – *Heliyon* **5**: e02952, 2019.

Meng L.L., Song J.F., Wen J. *et al.*: Effects of drought stress on fluorescence characteristics of photosystem II in leaves of *Plectranthus scutellarioides*. – *Photosynthetica* **54**: 414-421, 2016.

Oukarroum A., El Madidi S., Strasser R.J.: Exogenous glycine betaine and proline play a protective role in heat-stressed barley leaves (*Hordeum vulgare* L.): A chlorophyll *a* fluorescence study. – *Plant Biosyst.* **146**: 1037-1043, 2012.

Pearcy R.W., Ehleringer J.: Comparative ecophysiology of C₃ and C₄ plants. – *Plant Cell Environ.* **7**: 1-13, 1984.

Petrova N., Paunov M., Stoichev S. *et al.*: Thylakoid membrane reorganization, induced by growth light intensity, affects the plants susceptibility to drought stress. – *Photosynthetica* **58**: 369-378, 2020.

Pšidová E., Živčák M., Stojnić S. *et al.*: Altitude of origin influences the responses of PSII photochemistry to heat waves in European beech (*Fagus sylvatica* L.). – *Environ. Exp. Bot.* **152**: 97-106, 2018.

Qi J., Song C.-P., Wang B. *et al.*: Reactive oxygen species signaling and stomatal movement in plant responses to drought stress and pathogen attack. – *J. Integr. Plant Biol.* **60**: 805-826, 2018.

Rane J., Babar R., Kumar M. *et al.*: Desiccation tolerance of Photosystem II in dryland fruit crops. – *Sci. Hortic.-Amsterdam* **288**: 110295, 2021.

Rejeb K.B., Abdelly C., Savouré A.: How reactive oxygen species and proline face stress together. – *Plant Physiol. Bioch.* **80**: 278-284, 2014.

Rodrigues J., Inzé D., Nelissen H., Saibo N.J.M.: Source-sink regulation in crops under water deficit. – *Trends Plant Sci.* **24**: 652-663, 2019.

Semida W.M., Abdelkhalik A., Rady M.O.A. *et al.*: Exogenously applied proline enhances growth and productivity of drought stressed onion by improving photosynthetic efficiency, water use efficiency and up-regulating osmoprotectants. – *Sci. Hortic.-Amsterdam* **272**: 109580, 2020.

Sharma A., Kumar V., Shahzad B. *et al.*: Photosynthetic response of plants under different abiotic stresses: A review. – *J. Plant Growth Regul.* **39**: 509-531, 2019.

Slama I.S., Abdelly C., Bouchereau A. *et al.*: Diversity, distribution and roles of osmoprotective compounds accumulated in halophytes under abiotic stress. – *Ann. Bot.-London* **115**: 433-447, 2015.

Souza R.P., Machado E.C., Silva J.A.B. *et al.*: Photosynthetic gas exchange, chlorophyll fluorescence and some associated metabolic changes in cowpea (*Vigna unguiculata*) during water stress and recovery. – *Environ. Exp. Bot.* **51**: 45-56, 2004.

Stirbet A., Lazár D., Kromdijk J., Govindjee: Chlorophyll *a* fluorescence induction: can just a one-second measurement be used to quantify abiotic stress responses? – *Photosynthetica* **56**: 86-104, 2018.

Strasser R.J., Tsimilli-Michael M., Srivastava A.: Analysis of the chlorophyll *a* fluorescence transient. – In: Papageorgiou G.C., Govindjee (ed.): *Chlorophyll *a* Fluorescence: A Signature of Photosynthesis. Advances in Photosynthesis and Respiration*. Pp. 321-362. Springer, Dordrecht 2004.

Strasser R.J., Tsimilli-Michael M., Dangre D., Rai M.: Biophysical phenomics reveals functional building blocks of plants systems biology: a case study for the evaluation of the impact of mycorrhization with *Piriformospora indica*. – In: Varma A., Oelmüller R. (ed.): *Advanced Techniques in Soil Microbiology. Soil Biology*. Vol. 11. Pp. 319-341. Springer, Berlin-Heidelberg 2007.

Sullivan C.Y.: Techniques for measuring plant drought stress. – In: Larson K.L., Eastin J.D. (ed.): *Drought Injury and Resistance in Crops*. Pp. 1-18. CSSA Special Publications, Madison 1971.

Wang Z., Li G., Sun H. *et al.*: Effects of drought stress on photosynthesis and photosynthetic electron transport chain in young apple tree leaves. – *Biol. Open* **7**: bio035279, 2018.

Xu Z., Zhou G., Shimizu H.: Plant responses to drought and rewetting. – *Plant Signal Behav.* **5**: 649-654, 2010.

Yusuf M.A., Kumar D., Rajwanshi E. *et al.*: Overexpression of γ -tocopherol methyl transferase gene in transgenic *Brassica juncea* plants alleviates abiotic stress: Physiological and chlorophyll *a* fluorescence measurements. – BBA-Bioenergetics **1797**: 1428-1438, 2010.

Zhou R., Kan X., Chen J. *et al.*: Drought-induced changes in photosynthetic electron transport in maize probed by prompt fluorescence, delayed fluorescence, P700 and cyclic electron flow signals. – Environ. Exp. Bot. **158**: 51-62, 2019.

Zushi K., Kajiwara S., Matsuzoe N.: Chlorophyll *a* fluorescence OJIP transient as a tool to characterize and evaluate response to heat and chilling stress in tomato leaf and fruit. – Sci. Hortic.-Amsterdam **148**: 39-46, 2012.

Zhou R., Kan X., Chen J. *et al.*: Drought-induced changes in photosynthetic electron transport in maize probed by prompt fluorescence, delayed fluorescence, P700 and cyclic electron flow signals. – Environ. Exp. Bot. **158**: 51-62, 2019.

Appendix. The definitions of the relevant energy fluxes and fluorescence parameters of the JIP-test used in this study as described by Stirbet *et al.* (2018).

Parameter	Definition
Technical fluorescence parameters	
$F_v = F_m - F_0$	Maximum variable fluorescence
Efficiencies and quantum yields	
$ET_0/TR_0 = \psi E_0 = 1 - V_J$	The efficiency with which a PSII trapped electron is transported from Q_A^- to PQ
$RE_0/TR_0 = \psi R_0 = 1 - V_I$	Efficiency with which a PSII trapped electron is transported to PSI acceptors
$RE_0/ET_0 = \delta R_0 = \psi R_0 / \psi E_0$	Efficiency with which an electron from PQH_2 is transported to final PSI acceptors
Specific energy fluxes (per active PSII)	
$ABS/RC = (M_0/V_J) / \phi P_0$	Effective antenna size of active reaction centers
$TR_0/RC = M_0/V_J$	Maximum trapping per reaction center
$ET_0/RC = (M_0/V_J) \times \psi E_0$	The flux of electrons transported from Q_A^- to PQ
$DI_0/RC = ABS/RC - TR_0/RC$	The flux of energy dissipated per reaction center
Performance indexes	
$PI_{ABS} = (RC/ABS) \times [\phi P_0 / (1 - \phi P_0)] \times [\psi E_0 / (1 - \psi E_0)]$	Performance index on absorption basis
$PI_{ABS,total} = PI_{ABS} \times [\delta R_0 / (1 - \delta R_0)]$	Total performance index on absorption basis

© The authors. This is an open access article distributed under the terms of the Creative Commons BY-NC-ND Licence.